



Evaluation of self-cleaning photocatalytic paints: Are they effective under actual indoor lighting systems?



A. Galenda^{a,*}, F. Visentin^b, R. Gerbasi^a, M. Favaro^a, A. Bernardi^c, N. El Habra^a

^a CNR-ICMATE Institute of Condensed Matter Chemistry and Technologies for Energy, Italian National Research Council, Corso Stati Uniti, 4, 35127 Padova, Italy

^b Department of Industrial Engineering, University of Padova, Via Gradenigo, 6/a, 35131 Padova, Italy

^c CNR-ISAC Institute of Atmospheric Sciences and Climate, National Research Council, c/o Corso Stati Uniti, 4, 35127 Padova, Italy

ARTICLE INFO

Keywords:
Photocatalysis
Titanium dioxide
Self-cleanings
Indoor paints
Visible light

ABSTRACT

The aim of the paper is to assess the photocatalytic performance of self-cleaning paints – available in the market – designed for applications in indoor environment. Three self-cleaning photocatalytic paints were deeply characterised by means of complementary analytical techniques (X-Ray Diffraction, Thermogravimetry, Fourier Transform Infrared Spectroscopy in reflection mode and Absorption UV-vis Spectroscopy). In addition, the photocatalytic properties of the paints were tested accordingly to ISO 10,678 and ISO 2197-1 standards and in ad-hoc planned tests to evaluate their ability in methyl red and methylene blue bleaching under UVC, Xenon (with and without UV-400 filter), fluorescent and LED lamps exposure. To the best of our knowledge, this is the first paper dealing with the photocatalytic activity tests of indoor commercial self-cleaning paints under actual indoor light. Although restricted to the three investigated paints, the outcomes suggest that all samples are scarcely active under visible light and the pollutant probes are selectively bleached thanks to their sensitising effect. Consequently, the pollutants ability in injecting electrons in the TiO₂ conduction band deeply affects their removal. The paper highlights the requirement for an improved photocatalytic paint formulation with visible light active photocatalysts as well as the need of adequate ISO standards for visible light driven activity tests.

1. Introduction

The awareness of a healthy living environment is increasing in recent years and it concerns either outdoor or indoor locations. Recently, buildings and indoor living spaces have often been objects of dedicated studies aiming to optimise the energy demand in relation to heating and ventilating systems, as well as Indoor Air Quality (IAQ) management [1,2]. Designers and architects tend to limit the air mass exchanges with outdoor environment in order to minimise the energy demand for air conditioning, thus preferring the recycling of indoor air [3]. This involves the gradual increase in indoor pollutants and the decay in IAQ. The pollutants content in indoor spaces often reaches concentration higher than outdoor, thus requiring the introduction of adequate control and remediation systems in order to maintain a suitable air quality [4]. The main indoor air pollutants are usually particulate matters (PM), nitrogen oxides (NO_x), carbon monoxide (CO) and volatile organic compounds (VOCs) [5–7] that are produced by different sources like the adhesives and building materials' emission, the combustion processes as well as the use of household products, furniture, electric and electronic devices [8]. Skin and mucous membranes easily adsorb

VOCs, which eventually induce damages to organs and metabolic systems or asthma and cardiovascular illnesses and are renowned for being linked to the Sick Building Syndrome (SBS) [4]. Finally yet importantly, the indoor VOC limits are not yet unambiguously set due to the wide number of chemicals involved, and the relevant guidelines differ from country to country [8]. The European Scientific Committee on Occupational Exposure Limits (SCOEL) [9] establishes the limits for several VOCs and hazardous chemicals in the workplaces but no clear indications can be easily found regarding domestic environments. To the best of our knowledge, some non-official reports indicate that a Total VOC (T-VOC) content lower than 200 µg/m³ can be assumed as a good limit for preventing irritations or discomfort symptoms. 200–3000 µg/m³ can lead to irritation and/or discomfort; in 3000–25,000 µg/m³ range discomfort and headache are possible, while over 25,000 µg/m³ the toxic range is reached. However, these limits are often not useful, since the effect of specific chemicals can be evident at very different concentrations (as an example, the 8-h TLV-TWA (threshold limit value – time weighted average) limit by SCOEL is 369 µg/m³ for formaldehyde) and an ad-hoc study should be carried out for each specific compound.

Several remediation systems are available and indoor pollutant

* Corresponding author.

E-mail address: alessandro.galenda@cnr.it (A. Galenda).

removal takes currently advantage of various technologies. Air filtration through filtering and/or adsorbing cartridges is often used, nevertheless this simple procedure need a periodic cartridges replacement-regeneration (thus producing new wastes) and an ad-hoc ventilating system for the air circulation through the filters (i.e. the installation of the fan system and the energy consumption for the working operations) [8].

An alternative and low-cost VOCs remediation system is based on the Advanced Oxidation Processes (AOPs), thanks to the employment of suitable photocatalytic wall paints [10], which are usually also known as “self-cleaning”; thanks to their ability to self-remove organic dirty stains from their surface. A photocatalytic paint exploits the properties of a photocatalytic substance promoting the mineralisation of the volatile organic and inorganic pollutants compounds present in air or deposited on paint surface, thus obtaining carbon dioxide, water and inorganic inert salts as final products, improving the air quality and preserving the original aesthetic aspect. Briefly, in the photocatalytic process, a semiconductor is irradiated by photons with adequate energy, thus creating a couple of photo-electrons (e^-) and photo-holes (h^+) which can react with electron acceptors (O_2 as an example) and donors molecules, and initiating the oxidation process. Four main parameters affect the oxidation process, in particular: the catalyst amount, the photon wavelength, the concentration of the reactants and the radiation flux. Temperature does not deeply influence the catalyst performance if it is maintained in a room temperature range [11].

Dedicated scientific papers have always taken into account the performance of the photocatalysts themselves, but rarely the photocatalytic paint formulations have been characterised nor their performance accurately assessed in real or simulated indoor conditions [12–14]. The paint components, indeed, can significantly affect and modify the performance of the active photocatalytic compounds.

The self-cleaning photocatalytic paints can be designed for specific applications such as outdoor or indoor environments. In the latter case, the paint formulation should consider different light sources with respect to the outdoor one (i.e. the sun), with very different energy content for the activation of the photocatalytic compounds. Nevertheless, in the technical sheets of the paints under investigation, they are reported to be “active under artificial lights” and “effective without UV light”, while the specific lighting requirements for their activation are not reported.

The self-cleaning photocatalytic paint formulation, of course, is topic of industrial patents, but most of the indoor photocatalytic paint producers describe their products involving titanium dioxide, which is considered one of the most suitable photocatalysts because of its chemical stability, non-toxicity toward environmental and living species, low cost and wide availability [15]. Nevertheless, TiO_2 large band gap requires UV photons for the electrons-holes generation, while common and next future indoor artificial light sources emit low (energy saving fluorescent lamps) or almost no-UV radiations (LED lamps).

The aim of the present manuscript is to assess the performances in different conditions of three commercial indoor self-cleaning photocatalytic paints with respect to their photocatalytic performances in different conditions. The products have been analysed anonymously and the brand is intentionally not reported. The producers declare that the active paints are designed for indoor application and do not requiring UV radiation for their activation. The selected paints have been fully characterised and their photocatalytic performance has been investigated toward NO_x (i.e. for the indoor air quality improvement) and methylene blue removal (i.e. for self-cleaning action), according to the ISO standards 22197-1 [16] and 10678 [17] respectively. The ISO standards have been taken into account in order to provide an impartial evaluation of the paint performance, thus giving a benchmark for the comparison of the obtained results. Ad-hoc experiments were furthermore designed for testing their action in bleaching methyl red and

methylene blue stains under different light sources (UVC, Xenon, fluorescent and LED lamps).

The paint producers usually refer to the ISO standards for the certification of the photocatalytic properties and these protocols are generally planned under UVA light. This light source, however, is not used in the ordinary indoor conditions. Therefore, the paints were tested under prevalent indoor lights (fluorescent and LED lamps) in order to provide a valuable comparison with respect to more energetic sources. The recent ISO 19810:2017 standard [18] takes into account the use of visible light for testing the self-cleaning properties of photocatalytic materials. Nevertheless, this protocol prescribes the monitoring of the water contact angle (CA) as photocatalytic activity indicator. Unfortunately, the CA measurement cannot be performed on porous substrates (like the paints) that immediately absorb water.

2. Experimental

2.1. Materials

The three white (i.e. without any kind of colouring agent) commercial photocatalytic paints were kindly supplied by the manufacturers and used without any further modification. They were named in general terms as Self-Cleaning Paint 1–3, shortly “SCP-1”, “SCP-2” and “SCP-3”.

2.2. Measurements

The photocatalytic paints were characterised by complementary analytical techniques. The crystallographic structure was determined by X-Ray Diffraction (XRD) performed by means of a Philips X'Pert PW 3710 powder diffractometer operating in Bragg–Brentano θ – 2θ geometry mode, using $Cu K\alpha$ radiation ($\lambda = 0.154$ nm, 40 kV and 30 mA). Standard 2002 ICDD database files supported the phase identification.

The IR spectra were collected by a FT-IR Thermo-Nicolet IS10 spectrophotometer accumulating 32 scans at a resolution of 4 cm^{-1} . The samples were directly analysed in ATR mode (paint on glass slide). Moreover, a small amount of each commercial paint was treated with chloroform and the extract analysed in reflection mode with micro-IR (Thermo-Nicolet IS10 spectrophotometer coupled with Nicolet Continuum microscope) by FT-IR.

Thermogravimetric analyses (TG/DTA) were carried out under air atmosphere, with a heating rate of $5\text{ }^\circ\text{C}/\text{min}$ from room temperature up to $1200\text{ }^\circ\text{C}$, using the Netzsch STA 449 TG/DTA analyser.

The optical characterisation of the samples was performed with the Unicam UV500 spectrophotometer.

Each paint was deposited on microscope glass slides (1 mm in thickness was pursued in order to avoid any contribution by the holder material and thus observing only the actual paint effect) and dried in air for 24 h at room temperature (the paint homogeneity (absence of significant cracks) was checked by optical microscope at increasing magnitudes). The slides were then stained with $20\text{ }\mu\text{L}$ of methyl red (MR) or methylene blue (MB) solutions ($56\text{ }\mu\text{mol/L}$), dried in air at RT in dark conditions for 24 h and then exposed for 10 h to: UVC lamp (low pressure Hg lamp, total power 25 W , 750 lx , 10.5 W/m^2 in 220 – 280 nm range, 0.55 W/m^2 in 280 – 315 nm range, 0.30 W/m^2 in 315 – 400 nm range, 2.5 W/m^2 in 400 – 1050 nm range), Xenon lamp (5000 lx , with UV-400 filter – 0.001 W/m^2 in 220 – 280 nm range, 0.0005 W/m^2 in 280 – 315 nm range, 0.072 W/m^2 in 315 – 400 nm range, 23.6 W/m^2 in 400 – 1050 nm range and without UV-400 filter 0.0013 W/m^2 in 220 – 280 nm range, 0.001 W/m^2 in 280 – 315 nm range, 0.135 W/m^2 in 315 – 400 nm range, 23.9 W/m^2 in 400 – 1050 nm range), LED (500 lx , 0.0007 W/m^2 in 220 – 280 nm range, 0.0003 W/m^2 in 280 – 315 nm range, 0.0002 W/m^2 in 315 – 400 nm range, 1.2 W/m^2 in 400 – 1050 nm range) and fluorescent lamps (500 lx , 0.0009 W/m^2 in 220 – 280 nm range, 0.0004 W/m^2 in 280 – 315 nm range, 0.0033 W/m^2 in

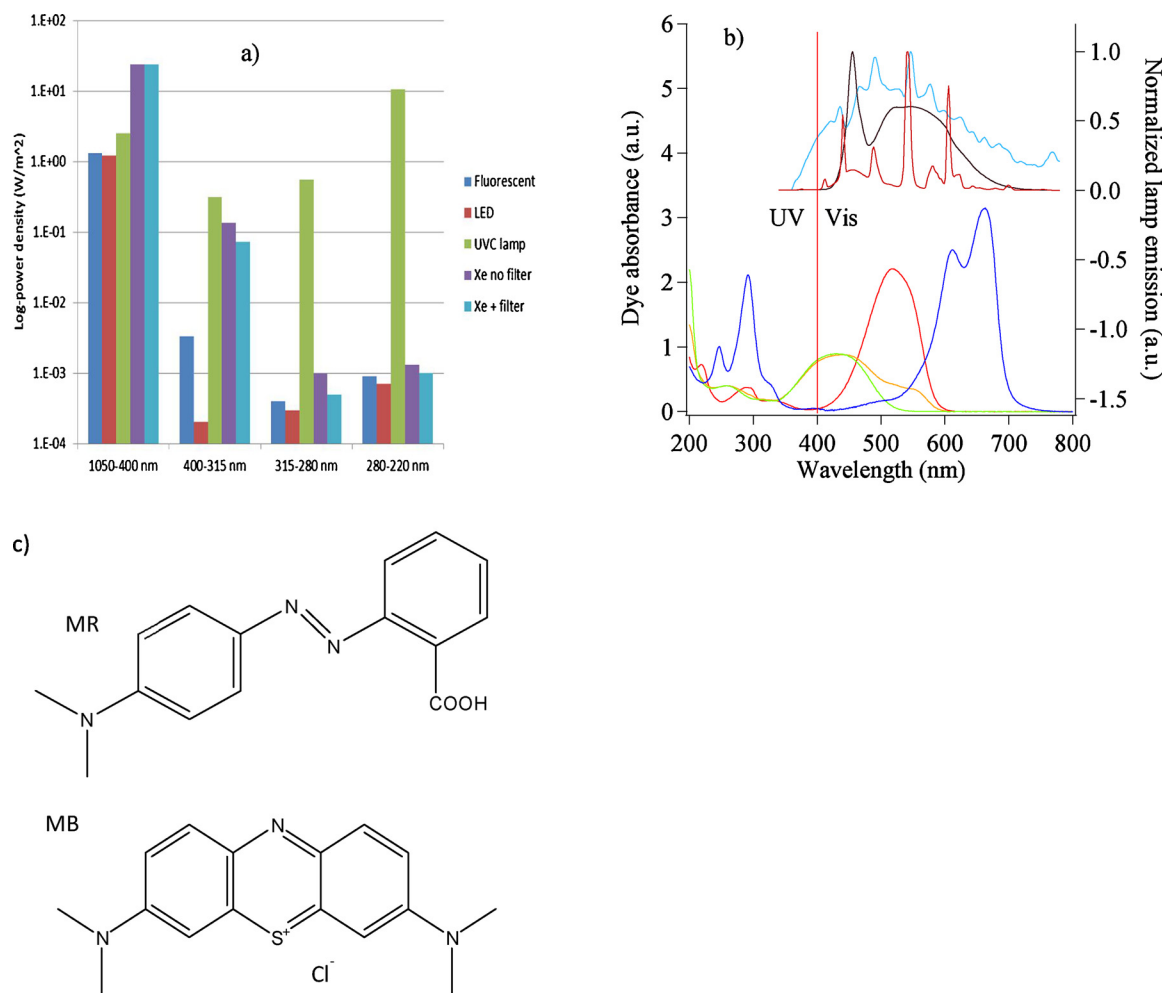


Fig. 1. (a) lamps power density characteristics (in logarithmic scale) under the experimental conditions; (b) absorption spectra of the investigated dyes (MR in acid condition (red), MR at native pH (orange), MR in basic condition (green) and MB (dark blue)) and emission spectra of the Xenon (light blue), fluorescent (brown) and LED employed lamps (black). The emission spectra are normalised with respect to their maximum and minimum values and shifted for a better comprehension; (c) chemical structures for methyl red and methylene blue (For interpretation of the references to colour in this figure legend, the reader is referred to the web version of this article).

315–400 nm range, 1.3 W/m^2 in 400–1050 nm range).

The power density data of the employed lamps was measured by Delta Ohm HD 2302.0 light-meter equipped with LP471RAD, LP471PA, LP471UVB and LP471UVC probes (Fig. 1a). The data were acquired by positioning the radiometer probes in the same position of the paint samples. The absorption spectra of the probe dyes – methyl red (MR) in acid, native and basic conditions and methylene blue (MB) – in comparison with the normalised emission spectra of the employed lamps are reported in Fig. 1b. These data allow a better comprehension of the dye absorption with respect to the lighting lamp, and then a better understanding of the dye bleaching. Fig. 1c shows the chemical structures of methyl red and methylene blue.

The characteristics of the coloured stains were monitored at predetermined times by mean of Konica-Minolta CM-700d digital spectrophotometer – colour-meter in $L^*\text{a}^*\text{b}^*$ reference system. The photo-bleaching without any photocatalytic paint was about 10% (in terms of ΔE) for MR under UVC and Xenon lamp (10 h exposure time); no significant bleaching was observed for MR under LED and fluorescent lamps and no photo-bleaching was observed for MB under any lamp. The temperature was set at 20 °C and RH at 50% ± 10%. Each test was performed three times on freshly prepared paint slides and freshly spotted dyes.

The photocatalytic and self-cleaning properties were finally tested under standard conditions by applying the ISO-22197-1 and ISO-10678 standards for the NO_x and MB abatement, respectively.

3. Results and discussion

3.1. Characterisation

The formulation of a paint is obviously object of patents or, at least, is an industrial secret to be safeguarded. The composition of the blend is specifically planned in order to obtain the best compromise among covering properties, scrub resistance, water vapour management, optical properties such as reflectance, opacity and lightness. A self-cleaning photocatalytic paint, moreover, also needs to provide a suitable condition for the best exploitation of the photocatalytic active compound. The characterisation of the paints is focused on the comprehension of their photocatalytic performance, while the painting properties (scrub resistance, covering and optical properties, etc.) is beyond the aim of the present manuscript and then not investigated.

3.1.1. Determination of pH

The pH of the commercial paints was determined by suspending 1 g of paint into 25 mL of distilled water and then measuring the pH by means of pH-meter. The results are summarised in Table 1. The determination of the environmental pH generated by the paint formulation is a very important parameter for understanding the photocatalytic performance with respect to the probe simulated pollutant. The first step in pollutant degradation by a photocatalytic material is its adsorption onto the photocatalyst surface. This kind of interaction is

Table 1

Water loss (wt.%) and thermogravimetric data for commercial compounds. PVAc and Acryl-PE indicates polyvinylacetate, and acrylic-polyester, respectively. The weight loss data from TGA are calculated from the TGA curve but referring to the starting (before desiccation) weight. The uncertainty on the data is $\pm 0.1\%$.

Sample	pH	18 h RT	24 h RT	15 h 110 °C	24 h 110 °C	H ₂ O desorption in TGA (RT-200 °C)	Organic fraction degradation (200–600 °C)	Inorganic fraction degradation (600–800 °C)
SCP-1	7.5	51.5	51.8	52.3	52.4	1.0	6.4 (PVAc)	4.5
SCP-2	5.5	40.9	41.2	42.4	42.4	1.8	13.7 (PVAc)	0.5
SCP-3	11.5	38.0	38.4	39.5	39.7	1.4	5.9 (Acryl-PE)	5.5

mainly electrostatic and it is related to the reciprocal state of charge (pollutant vs photocatalyst surface charge) [19–21]. Taking into account this consideration, the electrostatic interaction is optimised when opposite charges are involved (positive photocatalyst and negative pollutant or vice versa), and less intense when partial or concordant charges are present. Moreover, an acidic environment is advisable for photocatalytic process. The migration of photoelectron towards the compound surface is actually favoured if a positive charge is present at the surface (thus reducing the recombination of hole-electron pairs) [20]. It is important to point out that the strong basic environment in SCP-3 formulation could lead to worst photocatalytic performance because of a less efficient electron-hole separation.

3.1.2. Water content, thermal analysis and X-ray diffraction

Each commercial paint was carefully weighed and dried at room temperature and, later, at 110 °C in air in order to determine the water content. The weight variation was monitored after 18 and 24 h at RT, and after subsequent 15 and 24 h at 110 °C. The obtained results (Table 1) suggest that all paints lose most of their water content at the first measurement, in good agreement with their technical sheets concerning the curing time. The further forced desiccation step (110 °C) does not significantly modify the system conditions and does not lead to any kind of cracks.

The dried samples were then analysed by means of thermo-gravimetric analysis in order to evaluate the crystallisation water content and the organic-inorganic volatile fraction. The TG analyses were performed in air from RT to 1200 °C. Fig. 2 resumes the observed percent weight loss from RT to 800 °C (no significant events were evident from 800 to 1200 °C). The weight decrease from RT to about 200 °C is consistent with physisorbed and chemisorbed water desorption, while the subsequent decrease from 200 to about 600 °C can be ascribable to the organic fraction thermal degradation. Finally, from 600 to about 800 °C the decomposition-degradation of inorganic fraction (carbonate-like compounds decomposition, hydroxyl groups condensation) is observed. The residue amount is related to stable inorganic compounds. Table 1

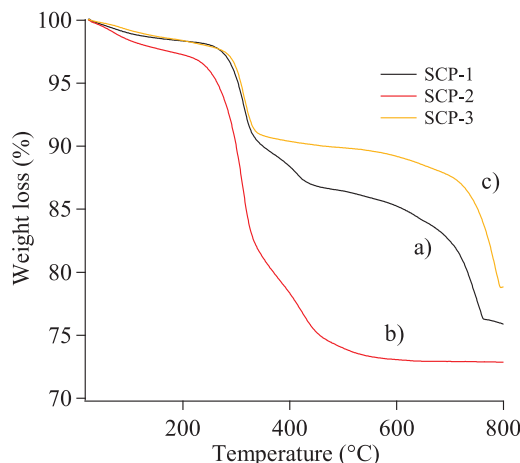


Fig. 2. TG results obtained for the commercial photocatalytic paints: (a) SCP-1 (black), (b) SCP-2 (red), (c) SCP-3 (orange) (For interpretation of the references to colour in this figure legend, the reader is referred to the web version of this article).

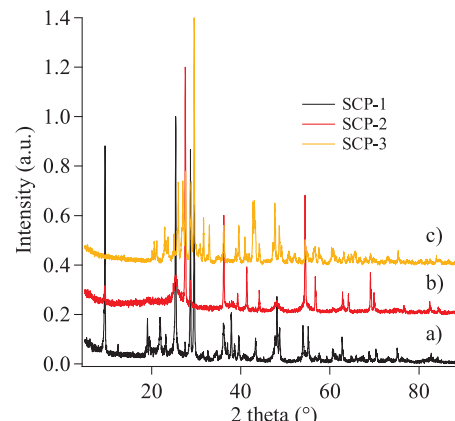


Fig. 3. XRD patterns obtained for the samples: (a) SCP-1 (black), (b) SCP-2 (red), (c) SCP-3 (orange). The spectra are normalised with respect to their maximum and minimum values and shifted for a better comprehension (For interpretation of the references to colour in this figure legend, the reader is referred to the web version of this article).

resumes the weight loss (wt.%) with the correspondent thermic events. The weight loss data from TGA are calculated from the TGA curve but referring to the starting (before desiccation) weight.

Dried paints have been finally investigated by means of X-Ray Diffraction (XRD) for identifying the inorganic fraction composition containing the active photocatalyst compound. The XRD patterns of the paints show the presence of signals from different species (Fig. 3): the identified compounds, their relative amount (with respect to the inorganic fraction only) and the crystallite dimensions of each identified phase are reported in Table 2. As stated by the technical sheets, all the self-cleaning paints have titanium dioxide as active photocatalyst, although in very different amount. SCP-1 contains about 23 wt.% TiO₂ (20% anatase – 3% rutile), SCP-2 about 70 wt.% (63% rutile, 7% anatase), while the SCP-3 has only 7 wt.% TiO₂ (100% rutile). This first information is fundamental when the photocatalytic performances will be analysed (see below). It is worth to underline, moreover, that all the TiO₂ phases have crystallites few tens of nanometres wide, which contributes to improve the catalytic properties with respect to micrometric crystallites. The paint formulation is then complemented by various amount of inorganic fillers (calcium carbonate, silicates, silica and barium sulphate), besides to the organic components, to achieve the final desired mechanical and optical characteristics.

Taking into account the gravimetric analysis and the XRD measurements, the SCP-1 composition is about 53 wt.% solvent (water) and 47 wt.% dry part, which is 1 wt.% rutile TiO₂, 8 wt.% anatase TiO₂, 31 wt.% inorganic fillers and 6 wt.% organic fillers. SCP-2 composition is 44 wt.% solvent (water) and 56 wt.% dry part, which is 27 wt.% rutile TiO₂, 3 wt.% anatase TiO₂, 13 wt.% inorganic fillers and 13 wt.% organic fillers, while SCP-3 is 41 wt.% solvent (water) and 59 wt.% dry part, which is 4 wt.% rutile TiO₂, 49 wt.% inorganic fillers and 6 wt.% organic fillers.

3.1.3. Infrared analysis

The dried samples (after the desiccation in the drying oven at 110 °C for 24 h) were ground and analysed by means of Fourier Transform

Table 2

XRD data and inorganic fraction composition. The relative percentages refer to the inorganic fraction only ($\pm 2\%$). The crystallites average dimensions (“D” in nm) obtained by Scherrer equation are also showed in parentheses.

Identified phases	ICDD card	SCP-1 wt. % (D)	SCP-2 wt. % (D)	SCP-3 wt. % (D)
Rutile (TiO_2)	03-065-0192	3 (29)	63 (62)	7 (51)
Anatase (TiO_2)	01-084-1286	20 (51)	6 (7)	
Calcite ($CaCO_3$)	01-072-1650	18 (44)		39 (58)
Talcum (Mg silicate)	01-083-1768	59 (54)		
Orthoclase (K-Al silicate)	01-075-1190			40 (38)
Barite ($BaSO_4$)	01-076-0213			14 (30)
Coesite (SiO_2)	01-072-1601		31 (45)	

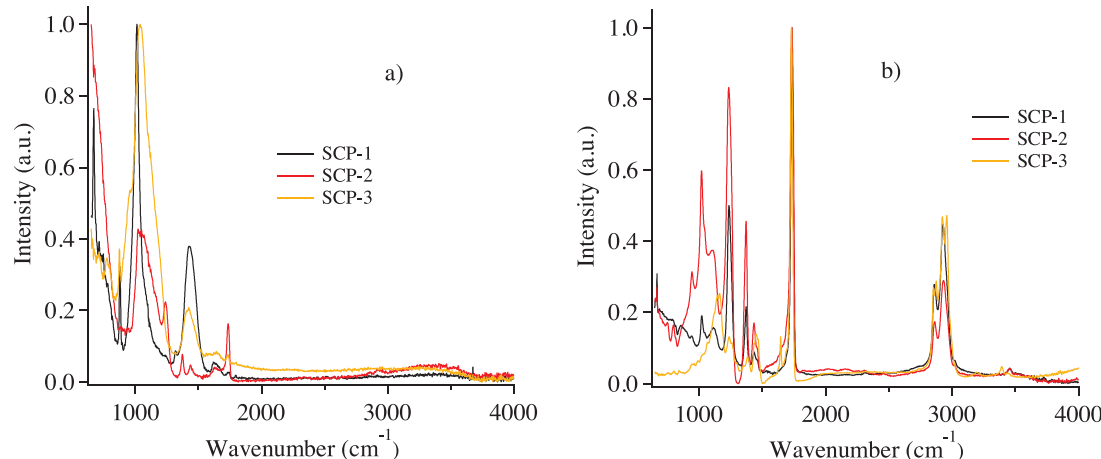


Fig. 4. IR spectra of the commercial paints. (a) ATR paint on slide, (b) chloroform extracted fraction by reflectance micro-IR mode (For interpretation of the references to colour in this figure legend, the reader is referred to the web version of this article).

Infrared spectroscopy (FT-IR) and evaluated by means of the instrumental software (OMNIC 8.2.0.387 by Thermo Fisher Scientific and “Database of ATR-FT-IR spectra of various materials” [22], NIST Database [23] and RRFUFF Database [24] as well as literature references [25–28]). The spectra directly obtained in ATR mode from the dried paints (Fig. 4a) well agree with the XRD results.

From the SCP-1 spectrum, indeed, typical Si–O signals are evident at 670 and 1010 cm^{-1} for talcum, while calcium carbonate presence is evident from the peaks at 874 and 1425 cm^{-1} . Concerning SCP-2, the absorption at the lowest wavenumbers is ascribable to rutile, while the Si–O bond gives signals at 670 and 1022 cm^{-1} . SCP-3 spectrum shows Si–O signal at 1040 cm^{-1} from orthoclase [25], at 874 and 1422 cm^{-1} from calcite and 1065 cm^{-1} (shoulder) for barium sulphate. In order to better highlight the organic fraction IR contributions, the fresh paints were treated with chloroform for extracting the organic compounds. The spectra obtained in reflectance by micro-IR mode on the chloroform-extracted fraction (Fig. 4b) suggest that the main component of the organic fraction in SCP-1 and SCP-2 is polyvinylacetate (PVAc) [26], while SCP-3 contains a blend acrylic-polyester based polymer (Acryl-PE) [27,28].

In summary, the results obtained from the IR characterisation further confirm the presence of commonly used fillers and pigments (talcum, calcium carbonate, silicate-based compounds, barium sulphate), while the analyses on the chloroform extracted fractions suggest the presence of typical binder resins in good quality paints (acrylics, polyesters and polyvinylacetate).

3.1.4. UV-vis light absorption characterisation

The ability of each paint in absorbing-reflecting ultraviolet and visible light was investigated in order to evaluate the lighting requirements for the activation of the photocatalytic process. The UV-vis absorption spectra of the commercial paints were collected and reported in Fig. 5a. The spectra clearly indicate that the main absorption

of the paints occurs in the UV zone, below 400 nm. Nevertheless, SCP-2 and SCP-3 spectra show a small absorption tail until about 415 and 405 nm, respectively. This suggests that SCP-2 and SCP-3 can also exploit a very small amount of the visible light. Fig. 5b shows the typical L*a*b* reference system: as evident, each colour can be identified as an L*a*b* coordinate set. In detail, the L* coordinate can vary from 0 (black) to 100 (white), the a* coordinate from -50 (green) to +50 (red), while the b* coordinate varies from -50 (blue) to +50 (yellow). The coordinates of each self-cleaning paint was measured by the colourmetre in order to provide their exact colour. SCP-1 gives: L* 96.59, a* -0.35, b* 1.30; SCP-2: L* 95.79, a* -0.34, b* 3.55, while SCP-3: L* 95.21, a* -0.82, b* 1.69. The results indicate that all paints have high “white” characteristics (each L* is close to 100); the paints also have a negligible tendency to the green (slightly negative a* values), while the deviation towards yellow (positive b* values) well agree with the absorption spectra. SCP-2, indeed, shows the more marked b* deviation with respect to the ideal zero, thus resulting in a slightly pale yellow paint, almost undetectable by human eye. It is worth to mention that a pure white paint is ineffective under visible light and, at least, a small absorption at the beginning of the visible range (i.e. a yellowish colour) is necessary for guaranteeing visible-active photocatalytic paints.

3.2. Photocatalytic tests

The use of a photoactive paint on indoor walls can capitalise both indoor air cleaning and energy saving. As described in the introduction section, a photocatalytic paint acts as adsorbent for volatile organic compounds and catalyses their mineralisation thus obtaining carbon dioxide and water as ideal final products. Following the same mechanism, dirt stains on paint surface can also be self-cleaned. During days, the indoor environments can be naturally lighted by sunlight, that provide infrared, visible and about 5% UVA radiation. Nevertheless, during dark periods or for those rooms not directly exposed to sun,

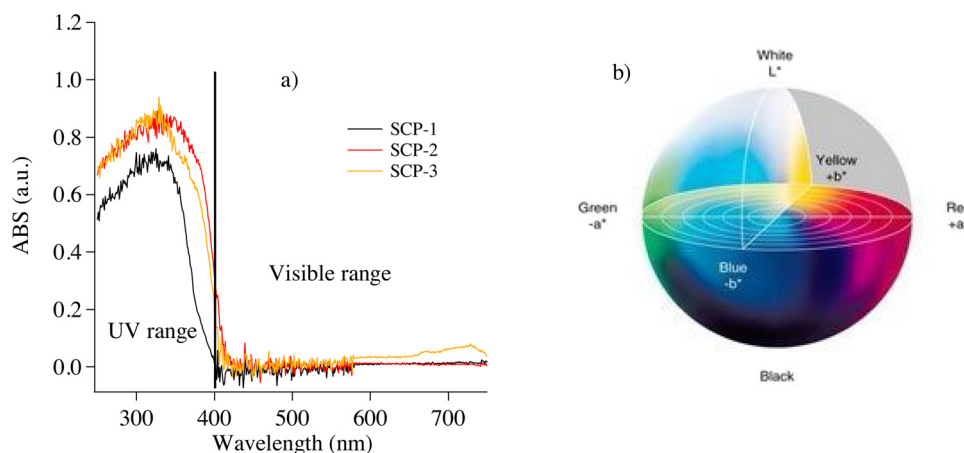


Fig. 5. (a) UV-vis absorption spectra for commercial paints. (b) $L^*a^*b^*$ reference system (For interpretation of the references to colour in the text, the reader is referred to the web version of this article).

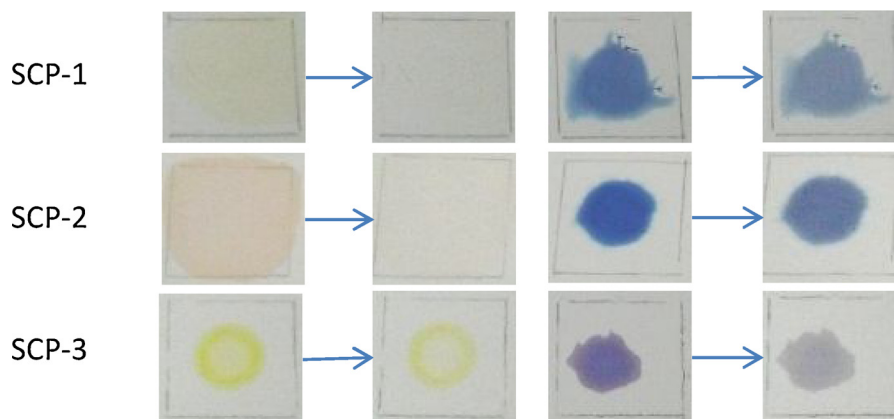


Fig. 6. Methyl Red (on the left) and Methylene Blue (on the right) bleaching on self-cleaning paints after exposure to UVC lamp for 10 h (For interpretation of the references to colour in this figure legend, the reader is referred to the web version of this article).

artificial light is the only available source. Commonly employed artificial lights are mainly fluorescent energy-saving lamps or, recently, LEDs. LEDs, indeed, are progressively replacing fluorescent and halogen lamps because of their lower energy consumption and longer lifetime. Fluorescent and LED lamps emit very low amount or no UV radiation and therefore photocatalytic paints could result poorly or completely ineffective.

The three paint activities are investigated under UVC, Xenon (with and without UV-400 filter), fluorescent and LED lamps in order to provide a complete set of data for their effectiveness. The Xenon lamp was chosen to mimic the conditions of an internal wall illuminated by the sun throughout a window. With more detail, it can simulate the lighting through an open window (without the UV-400 filter) or through a close window (with the UV-400 filter on, then with a reduced UV availability). The photocatalytic compounds are also tested under UVC radiation. The employed UVC lamp has its maximum emission at 254 nm, thus providing a high-energy radiation to the photocatalyst. The experiments under UVC light are carried out in order to overtake the limitation of a low-energy and low intensity lamp (in terms of wavelength and light intensity), and allow the photocatalysts to work under the best condition, thus giving their best available performance.

Beyond the most suitable lighting source, another parameter that affects the photocatalytic performances of the compounds is the intensity of the incident radiation on the sample surface. Taking into account this consideration, the lighting rate is chosen in order to reproduce the usual lighting condition in a typical commercial environment and an illumination of 500 lx was finally chosen for the fluorescent and LED lamps. Concerning Xenon lamp, the direct solar

illumination, in a typical sunny day, is about 100,000 lx, while the lighting throughout a window is about 50000–70000 lx, depending on the window characteristics. The lighting rate for the Xenon lamp was selected to be 5000 lx as a medium value between well and poor lighted zones during the daytime, also taking into account the oblique incident lighting with respect to a vertical wall.

The photocatalytic tests were carried out on the coloured stains described in measurement section, by monitoring their colour variation during exposure at light at predetermined times by mean of a digital colour-metre. The colour variation was determined by calculating the ΔE parameter, determined as specified in the following Eq. (1). The ΔE was successively expressed as percentage variation for a better comparison.

$$\Delta E = \sqrt{(L_2^* - L_1^*)^2 + (a_2^* - a_1^*)^2 + (b_2^* - b_1^*)^2} \quad (1)$$

The colour variation was always calculated with respect to the starting paint colour $L^*a^*b^*$ coordinates. In this way, the more the ΔE approaches to the 0% limit (and then coming back to the initial paint colour), the better the photocatalytic activity turns out to be.

Fig. 6 shows, as an example, the MR and MB bleaching after 10 h exposure to UVC light by the three self-cleaning paints. It is also worth to highlight the effect of the paint pH on methyl red. MR appears yellow-orange when deposited on SCP-1, red if deposited on SCP-2 and yellow on SCP-3, in good agreement with the acid-base properties of the paints.

Figs. 7 and 8 resume the obtained results under the different investigated conditions, while Table 3 resumes the dye colour removal

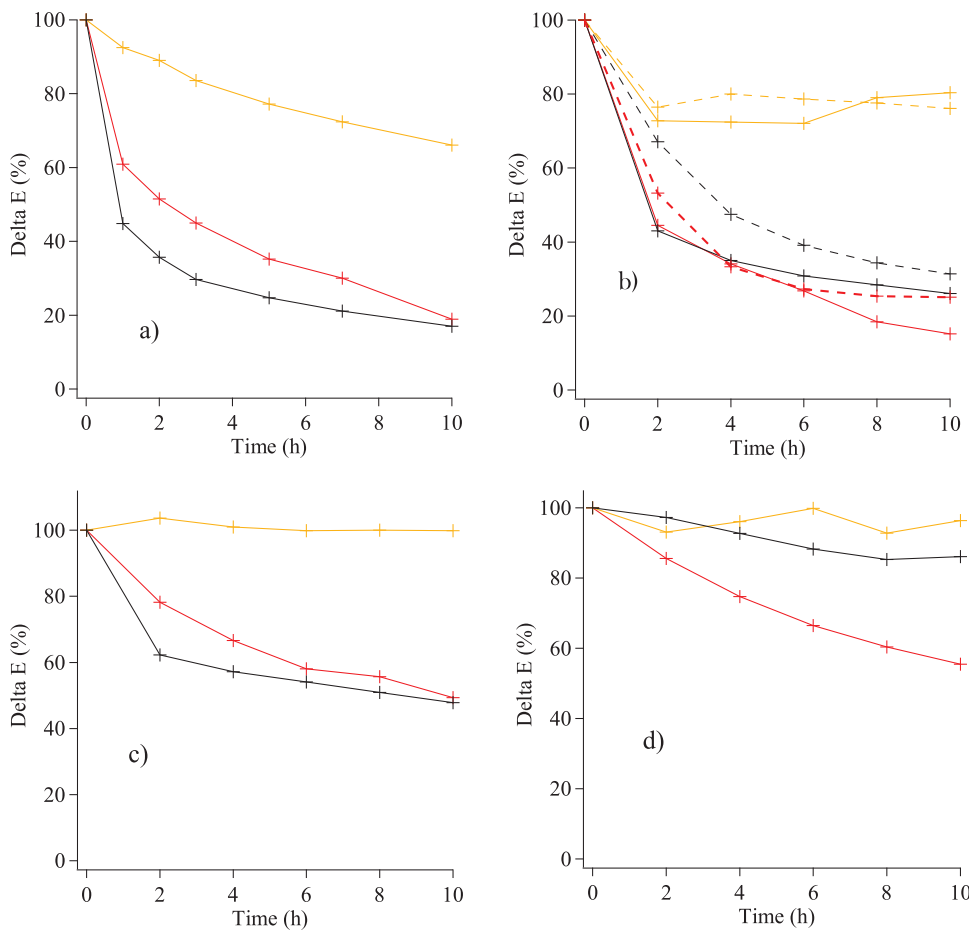


Fig. 7. ΔE variation (%) obtained for the commercial paints under different lighting systems for MR degradation. (a) UVC lamp; (b) Xenon lamp with (dashed lines) and without (solid lines) UV-400 filter; (c) fluorescent lamp; (d) LED lamp for 10 h exposure time. — SCP-1, — SCP-2, — SCP-3 (For interpretation of the references to colour in this figure legend, the reader is referred to the web version of this article).

percentage (complementary to 100 with respect to the ΔE % variation; all data have $\pm 4\%$ error) after 10 h exposure to different light sources. The performances of the investigated self-cleaning paints will be discussed under a double point of view: the former is related to the experimental conditions (i.e. the light sources), while the latter is with respect to their chemical composition.

Concerning the MR stains bleaching, the samples SCP-1 and SCP-2 give the best performance under all light sources, with SCP-2 equal or better than SCP-1. SCP-3 always gives the poorest results. In detail, the paint performance trends agree with the energy provided by the specific light source and the bleaching order is UVC > Xe (with no filter) > Xe (with filter) > Fluorescent > LED. UVC lamp of course provides the highest useful energy, nevertheless the Xenon lamp (without UV-400 filter) also leads to similar results (for SCP-1 and SCP-2), suggesting that the 254 nm wavelength from UVC lamp is not necessary (UVA is enough), and confirming the UV-vis absorption thresholds previously discussed (Fig. 4a); the presence of the UV-400 filter, thus essentially halves the UVA radiation, obviously reduces the SCP-1 and SCP-2 features. Fluorescent lamp leads to a further reduced activity. In this case the performance is affected by the lower light intensity (500 lx. for fluorescent vs 5000 lx for Xenon) and energy, that causes a lower number of generated electron-hole pairs. The LED lamp, finally, leads to the lowest MR bleaching. It is worth to notice that LED lamp appears as the most suitable benchmark for testing the performance of indoor photocatalytic paints, since this light technology is gaining the largest sales volumes in the marketplace. The absence of UV radiation in LED lamp (see Fig. 1b), indeed, requires the photocatalytic paint to be effective under pure visible light. In this condition, only SCP-2 maintains a significant, although reduced, response.

Methylene blue bleaching tests provide a completely different scenario: its degradation is less effective in comparison to methyl red

under all the investigated conditions. As for MR, also for MB the paint performance trends agree with the energy provided by the specific light source, but almost no activity can be detected under fluorescent and LED lamps. SCP-3 gives the best performance under UVC and Xenon light, while SCP-2 appears as the poorest, although it was basically the best with respect to MR.

The observed behaviours can be explained by taking onto account the specific photocatalyst-probe interactions. MR and MB have been chosen as probes because of their specific properties. Most authors agree that the probe adsorption onto the catalyst is a required step of the photodegradation process and that it is strongly influenced by surface-dye electrostatic interactions [19–21]. In this regard, the acid/base properties of both catalyst and organic dye should be known. MR, in detail, is a well-known pH-sensitive molecule and its net charge depends on the pH of the medium; the pKa for MR is 5.3 (as known, in basic solution the carboxylic group is dissociated (i.e. negative molecule), while in acid solution it is not ionised (neutral molecule); finally, in very acid solution the amino group can be protonated (positive molecule), see Fig. 1c for MR structure). Literature reports slightly different point of zero charge (pzc) values for titanium dioxide: from 5.1 to 6.8 [15,20,29–32]. At pH 5.3, the titania surface can be assumed to be almost neutral and 50% of MR will be ionised; in basic conditions titania surface is negatively charged as for MR. Finally, in acid solutions TiO_2 is positively charged, while MR tends to be neutral due to the protonation of the carboxylic group or positive if also the amino group is protonated. On the other hand, MB is a permanent cationic molecule (Fig. 1c). Thanks to the above-mentioned properties, and taking into account the paint pH values (see Table 1), MR is reasonably strongly adsorbed by SCP-2 and less intensely on SCP-1, while MR adsorption on SCP-3 appears negligible. Moreover, the specific MR absorption coefficient in its red appearance (acid form, on SCP-2) is more than twice

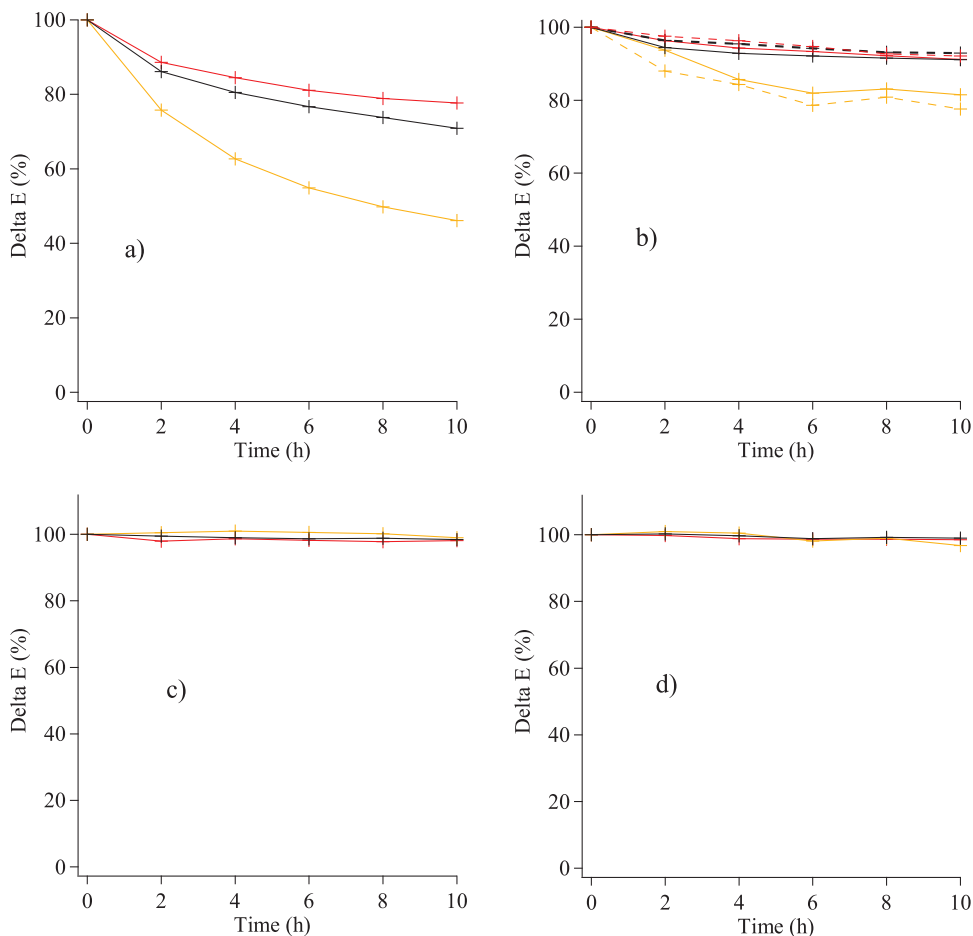


Fig. 8. ΔE variation (%) obtained for the commercial paints under different lighting systems for MB degradation. (a) UVC lamp; (b) Xenon lamp with (dashed lines) and without (solid lines) UV-400 filter; (c) fluorescent lamp; (d) LED lamp for 10 h exposure time. — SCP-1, — SCP-2, — SCP-3 (For interpretation of the references to colour in this figure legend, the reader is referred to the web version of this article).

Table 3

Methyl red (MR) and methylene blue (MB) colour removal percentage (complementary to 100 with respect to the ΔE % variation; all data have $\pm 4\%$ error) after 10 h exposure to different light sources for the investigated samples. MR = methyl red, MB = methylene blue.

Condition	SCP-1 10 h	SCP-2 10 h	SCP-3 10 h
Dye colour removal percentage (complementary to 100 with respect to ΔE % variation)			
MR-UVC	83	81	34
MR-Xe no UV filter	74	85	20
MR-Xe UV filter	67	75	24
MR-fluorescent	52	51	1
MR-LED	14	45	4
MB-UVC	29	22	54
MB-Xe no UV filter	9	9	19
MB-Xe UV filter	7	8	22
MB-fluorescent	2	2	1
MB-LED	1	2	1

with respect to the yellow one (on SCP-1 and SCP-3), thus further enhancing the light absorption.

MB is ostensibly well adsorbed only on SCP-3, while the interaction with SCP-1 and SCP-2 are less intense or negligible.

The photoactivity under LED, fluorescent and Xenon with UV-400 filter lights (i.e. essentially under visible or reduced UV light content) deserves a dedicated discussion since no, or a negligible amount, of UV radiation is emitted by these light sources. Since pure titanium dioxide, both in rutile and anatase form, is completely inert under visible light [15], special precautions need to be taken into account if the TiO_2 -containing photocatalytic paint is declared for UV-free usage (such as the use of ad-hoc doped TiO_2). As discussed above concerning UV-Vis

absorption measurements (Fig. 5a), SCP-1 shows no absorption in visible range, while SCP-2 and SCP-3 give a limited one. By these data, no pure photocatalytic phenomena are possible for SCP-1 and only a reduced photoactivity is conceivable for SCP-2 and SCP-3. Under these considerations, the activity in MR bleaching can be essentially ascribable to the MR sensitisation action, namely it is related to the initial light absorption by the dye, followed by electron injection from the dye to the TiO_2 conduction band [33–35]. The MR sensitisation mechanism effectiveness agree with the light source intensity and the Xenon lamp (5000 lx , 23.6 W/m^2 in visible range) is more efficient than fluorescent or LED (500 lx , 1.3 W/m^2 for fluorescent and 1.2 W/m^2 for LED in visible range).

The MB case appears more complicated. A large number of authors suggest that MB acts as sensitising antenna in photocatalytic test under visible light [36–38]. Concerning the visible range, in the present case MB bleaching was observed only under Xenon with UV400 filter, while almost no activity is detected for fluorescent and LED lamps. It is worth to point out that a longer experiment time (not shown for sake of brevity) leads to a slight increase in MB bleaching, reaching about 5% in 24 h. Actually, MB seems to be a very less efficient sensitising agent for TiO_2 with respect to MR and the low energy – low intensity fluorescent and LED lamps give no significant results.

In this case, Fig. 1b helps in understanding the reciprocal absorption properties of the dyes and the emission characteristics of the employed lamps. In detail, concerning the visible range, MR shows characteristic absorption spectra as a function of the pH. In acidic condition (example on SCP2 paint), MR appears red-violet with the maximum absorption at 518 nm, while it is yellow in basic conditions (on SCP-3, absorption at 428 nm) and orange at native pH (on SCP-1, absorption at about 440 nm). MB absorption, on the other hand, is basically pH independent

Table 4

Percentages of the totally emitted light by LED, Fluorescent and Xenon lamps in the methyl red and methylene blue absorption ranges (ranges amplitude = FWHM of the dye absorption bands).

	LED	Fluorescent	Xenon
MR 472–564 nm	44	46	34
MR 368–486 nm	26	29	28
MR 369–513 nm	37	38	39
MB 590–683 nm	21	22	21

and shows a composite band at 663 nm. **Table 4** summarises the percentage of the emitted light by each lamp in the range of the dye absorption. More in detail, the emission of each lamp was numerically integrated in the dye absorption range, taking the FWHM of the dye absorption band as extreme integration limits. The obtained data support the higher MR absorption from LED, fluorescent and Xenon lamps with respect to MB one (good superimposition of the MR absorption and lamps emission spectra, poor for MB), thus confirming the lower antenna effect of MB and its consequent lower bleaching.

Moreover, the paint white colour was also constantly monitored (the measures were performed in an area free from the dye stains but lighted by lamps) in order to evaluate its possible variation (ageing) as a consequence of the light exposure. No significant variation with respect to the initial “white” L*a*b* parameters have been detected after the photocatalytic tests.

The photocatalytic properties of the three commercial self-cleaning photocatalytic paints have also been analysed with respect to the ISO standard 10678 [17] for methylene blue and 22197-1 [16] for NO_x removal.

For sake of brevity, the detailed description of the standard procedures and apparatus is here omitted and the reader can refer to the ISO norms themselves [16,17] and to Da Silva et al. [39], Angelo et al. [40], Tawari et al. [41], Motola et al. [42] and Mills et al. [43] for further details.

Briefly, the ISO 10678 regulates the determination of photocatalytic activity of surfaces in aqueous medium by degradation of methylene blue. The results are given, as required, in terms of specific photoactivity P_{MB} (mol m⁻² h⁻¹) and photonic efficiency ζ_{MB} (%), calculated by the equations provided in the norm. The standard imposes the use of UVA lamp in the range 320–400 nm (370 in the present case) with 10 ± 0.5 W/m² measured at the height of the sample. The measurements were performed at 22 °C, in a beaker filled with 50 mL MB solution (10 μmol/L for test solution and 20 μmol/L for conditioning solution); sample surface = 6.25 cm².

The ISO 22197-1 specifies a test method for air purification (removal of nitric oxide) performance of semiconducting photocatalytic material. The analyses were performed as required by the norm protocol and the paint was supported on aluminium slabs with surface of 50 cm².

The measurements were carried out following the standard protocol, as well as the data collection and processing; the obtained outcomes are resumed in **Table 5**, where it is shown that all the investigated paints show general low activity and only SCP-1 shows a better behaviour, while SCP-3 appears to be the worst. Since no

literature data are available for commercial photocatalytic paints, the obtained outcomes cannot be directly compared with similar compounds but only with other photocatalytic materials. Concerning MB degradation, Da Silva et al. [39] found quite close results for Nb₂O₅ doped TiO₂, while Moser et al. [44] found specific photoactivities from 5 to 10 times lower than the investigated paints. Concerning the NO_x removal, the comparison with references [40,41] among the conversion yield, underlines the reduced performances of the investigated samples. The limited activities observed in NO_x removal lead to hypothesise that a reduced improvement can be obtained also with respect to the air quality enhancement in terms of VOCs reduction.

A brief discussion can be carried out about the fractional recovery (see **Table 5**). Since the aim of the photocatalyst is the complete mineralisation of the pollutants, thus obtaining CO₂ and H₂O starting from organic compounds or inorganic salts when inorganic pollutants are treated, the fractional recovery represents the removed NO_x portion (molar fraction) converted in nitrite and nitrate that can be found on the sample surface after the test (the nitrite and nitrate content determination before the test was carried out as reference). If lower than one, only a fraction of oxidised salts are produced while if equal to one, the entire NO_x amount is mineralised. A value higher than one indicates that nitrogen-containing species on the sample are mineralised during the test (thus modifying the sample composition and pauperising the sample initial formulation). The outcomes suggest that SCP-1 allows a complete mineralisation, while SCP-2 produces about 30% of oxidised salts. Finally, SCP-3 loses a significant amount of nitrogen-containing species after the test, thus suggesting a gradual modification of the paint composition.

Despite the general low results, it is worth to observe that the activity trend for the three paints is the same for ISO 10678 (MB) and ISO 22197-1 (NO_x) (**Table 5**). This suggests that the best paint composition for self-cleaning action towards MB is also suitable with respect to NO_x removal, and indicates that an optimisation work was done by the producers in terms of chemical and physical properties [45]. Tests with MB, in detail, can be used as a “bridge” in analysing the results from ISO and bleaching tests: the data showed in **Tables 3 and 5**, in fact, emblematically underline that the specific interaction paint-pollutant and the paint specific activity are crucial for obtaining overall good performances. The results from SCP-3 deserve a specific discussion since it is the worst paint with respect to both ISO tests (and towards MB in particular – ISO 10678) but it appears as the best in MB bleaching tests under UVC and Xenon lamps (cf. **Fig. 8a** and b and data in **Tables 3 and 5**). This apparent paradox can be ascribed to the amount of adsorbed MB: in the bleaching test, in fact, the same MB amount was dosed on the three paints (about 1 nmol of MB, obtaining the stains showed in **Fig. 6**), while in the ISO 10678 procedure, the required conditioning step (MB pre-adsorption until prescribed condition is reached) led to highest MB adsorption on SCP-3 (about 1.6 μmol s), thus probably producing a shielding effect for the incoming photons and the resulting decrease in photoactivity. This observation also suggests that the self-cleaning action can be reduced if an excessive pollutant amount contaminates the paint surface.

The paint performances can also be discussed in terms of chemical properties. The characterisation section well underlines that all the investigated products contain titanium dioxide as active photocatalytic

Table 5

Photocatalytic performances under ISO 10678 and ISO 22197-1 standards.

Sample	ISO 10678			ISO 22197-1				
	Specific photoactivity P _{MB} (mol m ⁻² h ⁻¹)	Photonic efficiency ζ _{MB} (%)	Removed NO _x (μmol)	Generated NO ₂ (μmol)	Adsorbed NO _x (μmol)	Desorbed NO _x (μmol)	Fractional recovery	Conversion yield (%)
SCP-1	3.62·10-5	0.032	2.115	2.422	0.016	0.136	1.050	5.07
SCP-2	2.99·10-5	0.027	1.303	0.399	0.041	0.111	0.310	3.44
SCP-3	1.49·10-5	0.013	0.205	-0.128	0.046	0.120	2.270	0.53

species, while it is worth to underline that no information are available regarding the presence of possible dopants. SCP-1 contains 9 wt.% TiO₂ (1% rutile, 8% anatase), SCP-2 has 30 wt.% (27% rutile and 3% anatase) and SCP-3 has only 4 wt.% (all rutile). The pH generated by the paint also influences the performances because it affects the state of charge of the photocatalysts and of several pollutant molecules.

Under this point of view, SCP-1 and SCP-2 appear as the best investigated paints thanks to their overall chemical composition. In detail, SCP-1 has a lower TiO₂ percentage with respect to SCP-2 but the highest anatase content, which is more active than rutile [15]. SCP-3, finally, shows the poorest activity because of the lowest and less active rutile contained in its formulation. It is also worth to point out once again that the effectiveness of a photocatalyst is not an absolute value, but the specific interaction with the pollutant molecules leads the activity.

The aim of a photocatalytic paint should be to provide a self-cleaning action (i.e. the conservation of a clean appearance) and the air quality improvement (i.e. the removal of the air pollutants such as NO_x and VOCs). These two actions should be simultaneously pursued by a suitable photocatalyst and then strictly related one another. Under this conditions, the ISO test 22197-1 quantifies an aspect related to the photocatalytic property for air purification (NO_x removal), while the bleaching tests and the ISO 10,678 outcomes indicate the ability in self-cleaning (dyes removal). Although no direct tests were carried out on the air quality improvement under visible light, the outcomes from the ISO tests (i.e. reduced photoactivity under UVA light) can be useful in hypothesising a negative trend when visible light is employed. The negligible bleaching for MB and the reduced one for MR (thanks to its own absorption properties with respect to the light emitted by the lamps), indeed, suggest then a further reduced activity.

The present work underlines the general reduced photoactivity of the investigated paints under pure visible light. This aspect is probably due to a lack in testing standards and to the recent and rapid evolution of the light sources market (i.e. from halogen and fluorescent to mainly LED lights) with respect to the previously developed photocatalysts. A wide scenario of effective visible-light activated photocatalysts is available from literature [35], but their immediate implementation in photocatalytic indoor paints is not so straight for different reasons such as their health assess, availability and cost-to-results ratio. Despite the long elapsed time from the first works, photocatalysis is still increasing the number of published papers year by year, thus testifying the interest in the field and the ongoing research for improved photocatalysts. Paint producers are also strongly focused on the improvement of their products by adapting the paint formulation to the new prevalent light sources.

4. Conclusion

Self-cleaning photocatalytic paints for indoor applications have been fully characterised and tested to assess their performance. The investigations were performed on three commercial products. The results are obtained from the restricted number of samples should not be taken as a general indication of the performances of this kind of products. All the analysed paints contain titanium dioxide as prevailing active photocatalytic compound, although in different amount and different crystallographic forms (anatase and rutile) and several organic and organic fillers.

Photocatalytic tests were performed under different and complementary conditions taking into account the current indoor light sources. Only a restricted number of standard protocols are available for the photocatalytic activity evaluation of self-cleaning paints; all of them, but ISO 19810:2017, consider UV as light source to assess the performance of photocatalytic paints, disregarding whether they are intended for indoor or outdoor use. Therefore, we believe the evaluation of the photocatalytic indoor paint by means of the current suggested ISO protocols appears inadequate, since no significant amount of

UV light is available in indoor environment. New and improved ISO standards are desirable for a more accurate paint evaluation with respect to actual indoor light sources (especially LED). Moreover, no visible light absorbing probes should be employed to avoid misunderstanding of the actual photocatalytic paint action and the probe sensitising effect. In the present paper, the photocatalytic activity was assessed both under ISO standards (ISO 10678 and ISO 22197-1) and by home-made tests with respect to UVC, Xenon, fluorescent and LED lamps and different probes (methyl red and methylene blue). The obtained results showed that photocatalytic performances change as a function of the provided energy (both in terms of light wavelength and power density), reference probe and eventually by the chemical composition of the specific paint. It is clearly proved that photocatalytic action under visible light is very limited and the dye bleaching mainly proceeds through the sensitisation action of the adsorbed dye. This feature leads us to conclude that only some pollutants can be removed in indoor conditions by the analysed paints when LED or fluorescent lamps are used, depending on the pollutants-paint interaction and pollutant ability in injecting electrons in the TiO₂ conduction band. Moreover, the obtained results suggest the inadequacy of the investigated paints with respect to the modern lighting sources and a new developing step is mandatory by the paint producers and, of course, by the researches, in order to provide visible light active photocatalysts. On the other hand, customers should also take into account that a perfectly white paint cannot be photoactive under visible light and a compromise of, at least, a yellowish paint need to be accepted.

Acknowledgements

This work was partially funded by the European Union's Seventh Programme for research, technological development and demonstration under grant agreement No. 609180, Ecoshopping. Energy efficient & Cost competitive retrofitting solutions for shopping buildings. The authors acknowledge Dr. L. Nodari and Dr. A. Gambirasi for the FT-IR analyses and their helpful discussions.

References

- [1] M.W. Ahmad, M. Mourshed, B. Yu, Y. Rezgui, Computational intelligence techniques for HVAC systems: a review, *Build. Simul.* 9 (2016) 359–398.
- [2] J.W. Kim, W. Yang, H.J. Moon, An integrated comfort control with cooling, ventilation, and humidification systems for thermal comfort and low energy consumption, *Sci. Technol. Built Environ.* 23 (2017) 264–276.
- [3] Energy efficient & Cost competitive retrofitting solutions for shopping buildings -Ecoshopping. European Union's Seventh Programme for research, technological development and demonstration under grant agreement No. 609180. <http://ecoshopping-project.eu/> (Accessed 31 October 2017).
- [4] A. Mauduit, C. Raillard, V. Héquet, L. Le Coq, J. Sablayrolles, L. Molins, Adsorption phenomena in photocatalytic reaction: the case of toluene, acetone and heptane, *Chem. Eng. J.* 170 (2011) 464–470.
- [5] Y. Huang, S.S.H. Ho, Y. Lu, R. Niu, L. Xu, J. Cao, S. Lee, Removal of indoor volatile organic compounds via photocatalytic oxidation: a short review and prospect, *Molecule* 21 (2016) 56–76.
- [6] WHO guidelines for indoor air quality: selected pollutant, ISBN 978 92 890 0213 4, World Health Organization Regional Office for Europe, Scherfigsvej 8, DK-2100, Copenhagen, Denmark (2010).
- [7] A.H. Mamaghani, F. Haghigiat, C. Lee, Photocatalytic oxidation technology for indoor environment air purification: the state of the art, *Appl. Catal. B* 203 (2017) 247–269.
- [8] A. Luengas, A. Barona, C. Hort, G. Gallastegui, V. Platel, A. Elias, A review of indoor air treatment technologies, *Rev. Environ. Sci. Biotechnol.* 14 (2015) 499–522.
- [9] Health and safety at work – Scientific Committee on Occupational Exposure Limits. <http://ec.europa.eu/social/main.jsp?catId=148&langId=en&intPageId=684> (Accessed 31 October 2017).
- [10] V. Binias, D. Venieri, D. Kotzias, G. Kiriakidis, Modified TiO₂ based photocatalyst for improved air and health quality, *J. Materomics* 3 (2017) 3–16.
- [11] M.N. Chong, B. Jin, C.W.K. Chow, C. Saint, Recent developments in photocatalytic water treatment technology: a review, *Water Res.* 44 (2010) 2997–3027.
- [12] C. George, A. Beeldens, F. Barmpas, J.F. Doussin, G. Manganelli, H. Herrmann, J. Kleffmann, A. Mellouji, Impact of photocatalytic remediation of pollutants on urban air quality, *Front. Environ. Sci. Eng.* 10 (5) (2016) 02.
- [13] C. Giosù, A. Belli, A. Mobili, B. Citterio, F. Biavasco, M.L. Ruello, F. Tittarelli, Improving the impact of commercial paint on indoor air quality by using highly porous fillers, *Buildings* 7 (2017) 7–22.

[14] J. Kolarik, J. Toftum, The impact of a photocatalytic paint on indoor air pollutants: sensory assessments, *Build. Environ.* 52 (2012) 396–402.

[15] O. Carp, C.L. Huisman, A. Reller, Photoinduced reactivity of titanium dioxide, *Prog. Solid State Ch.* 32 (2004) 33–177.

[16] ISO 22197-1: 2007, “Fine ceramics, advanced technical ceramics – test method for air purification performance of semiconducting photocatalytic materials – part 1: removal of nitric oxide”, ISO, Geneve (2007).

[17] ISO 10678: 2010, “Fine ceramics, advanced technical ceramics – determination of photocatalytic activity of surfaces in an aqueous medium by degradation of methylene blue”, ISO, Geneve (2010).

[18] ISO 19810:2017. “Fine ceramics (advanced ceramics, advanced technical ceramics) – Test method for self-cleaning performance of semiconducting photocatalytic materials under indoor lighting environment – Measurement of water contact angle.

[19] A. Galenda, L. Crociani, N. El Habra, M. Favaro, M.M. Natile, G. Rossetto, Effect of reaction conditions on methyl red degradation mediated by boron and nitrogen doped TiO₂, *Appl. Surf. Sci.* 314 (2014) 919–930.

[20] R. Comparelli, E. Fanizza, M.L. Curri, P.D. Cozzoli, G. Mascolo, R. Passino, A. Agostiniano, Photocatalytic degradation of azo dyes by organic-capped anatase TiO₂ nanocrystals immobilized onto substrates, *Appl. Catal. B* 55 (2005) 81–91.

[21] M.N. Chong, B. Jin, C.W.K. Chow, C. Saint, Recent development in photocatalytic water treatment technology: a review, *Water Res.* 44 (2010) 2997–3027.

[22] http://lisa.chem.ut.ee/IR_spectra/ Database of ATR-FT-IR spectra of various materials (Accessed 31 August, 2017).

[23] NIST Chemistry WebBook, <http://webbook.nist.gov/chemistry/> (Accessed 26 February 2018).

[24] RRUFF Project website containing an integrated database of Raman spectra, X-ray diffraction and chemistry data for minerals, <http://rruff.info/> (Accessed 26 February 2018).

[25] F. Bosch-Reig, J.V. Gimeno-Adelnatado, F. Bosh-Mossi, A. Domenech-Carbò, Quantification of mineral form ATR-FTIR spectra with spectral interferences using the MRC method, *Spectrochim. Acta A* 181 (2017) 7–12.

[26] S. Wei, V. Pintus, M. Schreiner, Photochemical degradation study of polyvinyl acetate paints used in artworks by py-GC-MS, *J. Anal. Appl. Pyrol.* 97 (2012) 158–163.

[27] P.H. Pi, J. Chen, K. Chen, Z.Q. Cai, D.F. Zheng, X.F. Wen, J. Cheng, Z.R. Yang, Effects of acid treatment on adhesive performance of encapsulated aluminium pigments on plastic sheets, *Can. J. Chem.* 90 (2012) 1224–1230.

[28] K. Sethuraman, T. Lakshminandhan, M. Alagar, Surface free energy and dielectric properties of vinyltriethoxysilane functionalized SBA-15-reinforced unsaturated polyester nanocomposites, *Polym. Composite* 37 (2016) 3433–3441.

[29] M.R. Sohrabi, M. Ghavami, Photocatalytic degradation of direct red 23 dye using UV/TiO₂: effect of operation parameters, *J. Hazard. Mater.* 153 (2008) 1235–1239.

[30] I.K. Kostantinou, T.A. Albanis, TiO₂-assisted photocatalytic degradation of azo dyes in aqueous solution: kinetic and mechanistic investigations. A review, *Appl. Catal. B* 49 (2004) 1–14.

[31] T. Vescovi, H.M. Coleman, R. Amal, The effect of pH on UV-based advanced oxidation technologies – 1,4 – dioxane degradation, *J. Hazard. Mater.* 182 (2010) 75–79.

[32] D. Friedmann, C. Mendive, D. Bahnemann, TiO₂ for water treatment: parameters affecting the kinetics and mechanisms of photocatalysis, *Appl. Catal. B* 99 (2010) 398–406.

[33] V. Gombac, L. De Rogatis, A. Gasparotto, G. Vicario, T. Montini, D. Barreca, G. Balducci, P. Fornasiero, E. Tonello, M. Graziani, TiO₂ nanopowders doped with boron and nitrogen for photocatalytic application, *Chem. Phys.* 339 (2007) 111–123.

[34] M. Rochkind, S. Pasternak, Y. Paz, Using dyes for evaluating photocatalytic properties: a critical review, *Molecules* 20 (2015) 88–110.

[35] N. Shaham-Waldmann, Y. Paz, Away from TiO₂: a critical minireview on the developing of new photocatalysts for degradation of contaminants in water, *Mater. Sci. Semicond. Proc.* 42 (2016) 72–80.

[36] A. Mills, J. Wang, Photobleaching of methylene blue sensitised by TiO₂: an ambiguous system? *J. Photochem. Photobiol. A* 127 (1999) 123–134.

[37] B. Ohtani, Photocatalysis A to Z – what we know and what we do not know in a scientific sense, *J. Photochem. Photobiol. C* 11 (2010) 157–178.

[38] X. Yan, T. Ohno, K. Nishijima, R. Abe, B. Ohtani, Is methylene blue an appropriate substrate for a photocatalytic activity test? A study with visible-light responsive titania, *Chem. Phys. Lett.* 429 (2006) 606–610.

[39] A.L. da Silva, M. Dondi, D. Hotza, Self-cleaning ceramic tiles coated with Nb₂O₅-doped TiO₂ nanoparticles, *Ceram. Int.* 43 (2017) 11986–11991.

[40] J. Angelo, L. Andrade, A. Mendes, Highly active photocatalytic paint for NO_x abatement under real-outdoor conditions, *Appl. Catal. A* 484 (2014) 17–25.

[41] A. Tawari, W.D. Einicke, R. Glasser, Photocatalytic oxidation of NO over composites of titanium dioxide and zeolite ZSM-5, *Catalysts* 6 (2016) 31–47.

[42] M. Motola, L. Satrapinskyy, T. Roch, J. Subrt, J. Kupcik, M. Klementova, M. Jakubickova, F. Peterka, G. Plesch, Anatase TiO₂ nanotube array and titania films on titanium mesh for photocatalytic NO_x removal and water cleaning, *Catal. Today* 284 (2017) 59–64.

[43] A. Mills, An overview of the methylene blue ISO test for assessing the activities of photocatalytic films, *Appl. Catal. B* 128 (2012) 144–149.

[44] E.M. Moser, S. Chappuis, J. Olleros, Production of photocatalytically active titania layers: a comparison of plasma process and coating properties, *Surf. Coat. Technol.* 227 (2013) 2–9.

[45] S.S. Lucas, J.L. Barroso de Aguiar, Multifunctional wall coating combining photocatalysis, self-cleaning and latent heat storage, *Mater. Res. Express* 5 (2018) 025702.